Journal of Cerebral Blood Flow & Metabolism (2015) 35, 74–85

www.jcbfm.com

OPEN

ORIGINAL ARTICLE

GLUT2-mediated glucose uptake and availability are required for embryonic brain development in zebrafish

Rubén Marín-Juez[1,3], Mireia Rovira[1], Diego Crespo[1,4], Michiel van der Vaart[2], Herman P Spaink[2] and Josep V Planas[1]

Glucose transporter 2 (GLUT2; gene name *SLC2A2*) has a key role in the regulation of glucose dynamics in organs central to metabolism. Although GLUT2 has been studied in the context of its participation in peripheral and central glucose sensing, its role in the brain is not well understood. To decipher the role of GLUT2 in brain development, we knocked down *slc2a2* (*glut2*), the functional ortholog of human GLUT2, in zebrafish. Abrogation of *glut2* led to defective brain organogenesis, reduced glucose uptake and increased programmed cell death in the brain. Coinciding with the observed localization of *glut2* expression in the zebrafish hindbrain, *glut2* deficiency affected the development of neural progenitor cells expressing the proneural genes *atoh1b* and *ptf1a* but not those expressing *neurod*. Specificity of the morphant phenotype was demonstrated by the restoration of brain organogenesis, whole-embryo glucose uptake, brain apoptosis, and expression of proneural markers in rescue experiments. These results indicate that *glut2* has an essential role during brain development by facilitating the uptake and availability of glucose and support the involvement of *glut2* in brain glucose sensing.

Journal of Cerebral Blood Flow & Metabolism (2015) **35,** 74–85; doi:10.1038/jcbfm.2014.171; published online 8 October 2014

Keywords: apoptosis; glucose uptake; hindbrain; neural progenitor cells; zebrafish

INTRODUCTION

Glucose represents the main energy source for many organisms and its cellular uptake is facilitated by passive diffusion glucose transporters (GLUTs). GLUTs are integral membrane proteins that contain 12 membrane-spanning helices with the amino and carboxyl termini exposed to the cytosol. Each GLUT isoform has a specific role in glucose metabolism as determined by its pattern of tissue expression, substrate specificity, transport kinetics, and regulated expression under different physiological conditions. Particularly, the intestine, endocrine pancreas, kidney, and liver, tissues that have key roles in carbohydrate metabolism, express GLUT2, a low-affinity transporter for glucose, fructose, mannose, and galactose, that is also a high-affinity transporter for glucosamine.[1] The ability of GLUT2 to transport different types of hexoses at a wide range of concentrations ensures fast equilibration of glucose between the extracellular space and the cell cytosol.[1] GLUT2 participates in the intestinal and renal absorption of glucose, the stimulation of insulin secretion by glucose in β-pancreatic cells and the entry and output of glucose by the liver. Mutations in the GLUT2 gene cause hepatorenal glycogen accumulation, nephropathy, and defects in glucose homeostasis in humans (i.e., Fanconi–Bickel syndrome; FBS).[2] In addition, GLUT2 is also expressed in the central nervous system, particularly in neurons and glial cells of brain areas known to participate in the central glucose sensing system that regulates glucose homeostasis and food intake.[3] In glial cells, GLUT2 is involved in the detection of hypoglycemia and has an important role mediating the counter-regulatory response to glucose deficit.[4] Evidence for the important role of GLUT2 in the regulation of feeding comes from observations indicating that individuals from two Canadian populations harboring a single-nucleotide polymorphism in the GLUT2 gene ($Thr^{110}Ile$) show abnormal sugar intake.[5] Similarly, abnormal feeding behavior has been observed by blocking GLUT2 intracerebroventricularly in rats,[6] in GLUT2- null mice,[7] or in GLUT2-SDD mice.[8] Unfortunately, to date, the neuronal functions of GLUT2 are poorly understood and the importance of GLUT2 during brain development is not known.

In the present study, we have used the developing zebrafish embryo model to examine *in vivo* the physiological role of *glut2*. The ease of genetic manipulation, rapid development, and optical transparency of the zebrafish embryo provide a unique opportunity to unravel the mechanisms following the perturbation of glucose homeostasis associated with loss of function of this transporter. Our findings indicate that abrogation of zebrafish *glut2 in vivo* results in severe abnormalities in the development of the brain and particularly in neural progenitor cells. These alterations are associated with impaired glucose uptake and a significant increase in cell apoptosis in the brain of morphant embryos. Our results support the notion of an important role of GLUT2 in the development of the brain, particularly in regions involved in glucose sensing.

[1]Departament de Fisiologia i Immunologia, Facultat de Biologia, Universitat de Barcelona and Institut de Biomedicina de la Universitat de Barcelona (IBUB), Barcelona, Spain and [2]Department of Molecular Cell Biology, Institute of Biology, Leiden University, Leiden, The Netherlands. Correspondence: Dr JV Planas, Departament de Fisiologia i Immunologia, Facultat de Biologia, Universitat de Barcelona, Av. Diagonal 643, 08028 Barcelona, Spain.
E-mail: jplanas@ub.edu
This work was supported by a grant from the Spanish Ministry of Science and Education CSD2007-0002 to JVP. RM-J, MR, and DC were supported by a predoctoral fellowship from the Spanish government, by a grant from Sudoe-Interreg-EU AQUAGENET, SOE2/P1/E287 to JVP and by grant CSD2007-0002, respectively.
[3]Present address: ZF-screens B.V., J.H. Oortweg 19, 2333 CH Leiden, The Netherlands.
[4]Present address: Division of Developmental Biology, Department of Biology, Faculty of Science, Utrecht University, Utrecht, The Netherlands.
Received 16 June 2014; revised 14 August 2014; accepted 12 September 2014; published online 8 October 2014

MATERIALS AND METHODS

Zebrafish Maintenance

Wild-type zebrafish of the AB/TL and Casper strains were handled following a procedure approved by the Ethical Committee of Animal Experimentation of the University of Barcelona and maintained according to standard protocols (http://zfin.org). Embryos were grown at 28.5 °C in egg water (i.e., water used to raise young embryos; 60 μg/mL Instant Ocean Sea Salts, Blacksburg, VA, USA).

Imaging

Embryos were examined with a Leica MZ16 FA fluorescence stereomicroscope and images were acquired with a DFC420C camera (Leica, Wetzlar, Germany) and Leica Application Suite 3.8 (LAS) Microscope Software. Pictures were analyzed using ImageJ 1.45 software (National Institutes of Health). TUNEL-positive cells were analyzed and quantified using Icy 1.2.4.1 bio-imagining software (www.bioimageanalysis.org).

In Situ Hybridization and Immunohistochemistry

Antisense probes were generated for zebrafish *glut2*[9] and for *pre-proinsulin*, *atoh1b*, *atoh1c*, *ptf1a*, and *neurod* that were amplified by PCR and subcloned into pGEM-T Easy vector (Promega, Barcelona, Spain). *glut2* was linearized with SpeI and *atoh1b*, *atoh1c*, *ptf1a*, and *neurod* were linearized with SalI and used as template for the generation of riboprobes using the DIG and Fluorescein labeling kits (Roche, Mannheim, Germany). For whole-mount immunostaining, zebrafish embryos were fixed in 4% paraformaldehyde and washed with PBS (pH7.4) containing 1% dimethyl sulfoxide (Merck, Darmstadt, Germany) and 0.3% Triton X-100 (Sigma-Aldrich, Alcobendas, Spain; phosphate-buffered saline-dimethyl sulfoxide-Triton X100 (PBS-DTx)) at room temperature. Embryos at 24 and 48 hours post fertilization (hpf) were digested with collagenase type IA (Sigma-Aldrich) diluted in PBS-DTx (1 mg/mL) at 37 °C for 10 and 20 minutes, respectively. Next, after 2 to 5 hours of incubation in blocking solution (PBS-DTx with 5% sheep serum) the specimens were incubated with an antibody against acetylated tubulin (Sigma-Aldrich) diluted (1:200) in blocking solution during 16 hours at 4 °C under slow stirring (30 to 50 rpm). Embryos were then washed thoroughly with PBS-DTx and incubated with the secondary antibody, goat anti-mouse Alexa-conjugated 488 diluted (1:500) in blocking solution for 12 to 24 hours at 4 °C. After extensive washing with PBS-DTx (pH7.4), the specimens were stored in PBS.

Morpholino Design and Injections

To knockdown zebrafish *glut2* expression, we designed antisense morpholinos targeting the translational start site (5′-ACTGCTTCTCCATTTTGCATG AAGT-3′) and the splice acceptor site of exon 6 (5′-ATGACCTGCAGAC AACAAGGACACC-3′). Morpholinos were reconstituted in RNAse-free water according to manufacturer's instructions (Gene Tools LLC, Philomath, OR, USA). Morpholinos targeting the translational start site (ATG MO) and the splice acceptor site (splice MO) were titrated at doses of 2.2 to 8.4 ng into single-cell embryos and the lowest effective dose was determined (3.1 ng) and used for all subsequent experiments. A standard control morpholino (5′-CCTCTTACCTCAGTTACAATTTATA-3′) (Gene Tools LLC) was used as negative control. Capped mRNAs were synthesized from rat and zebrafish GLUT2 full-length cDNAs cloned into pcDNA3 and pBK-CMV vectors, respectively, using mMessage mMachine kit (Life Technologies, Barcelona, Spain). Two hundred and fifty picograms per embryo of rat GLUT2 and 150 pg/embryo of zebrafish *glut2* mRNAs were co-injected with 3.1 ng/embryo of the ATG MO and the splice MO, respectively.

In Vivo Glucose Uptake Assay

Control and ATG morphants and rescued embryos were injected at 24 hpf in the yolk sac with 2.5 mg/mL 2-(*N*-(7-nitrobenz-2-oxa-1,3-diazol-4-yl) amino)-2-deoxyglucose (2-NBDG), a fluorescent glucose analog (Life Technologies), and incubated at 28.5 °C for 60 minutes. At the termination of the incubation period, seven embryos per condition were anesthetized with 3-aminobenzoic acid ethyl ester methanesulfonate (Sigma-Aldrich) and analyzed under a fluorescence stereomicroscope. The fluorescent signal was measured as described above. To visualize the transport of glucose, the embryos were embedded in 1% methylcellulose.

Detection of Cell Death

Cell death was detected *in vivo* using the vital dye acridine orange (acridinium chloride hemizinc chloride; Sigma-Aldrich). Embryos were dechorionated and incubated with acridine orange (5 μg/mL) for 30 minutes at 28.5 °C in the dark. At least seven embryos per condition were washed three times with egg water for 5 minutes and immediately visualized with a fluorescence stereomicroscope and the fluorescent signal was measured as described above. Apoptosis in zebrafish whole-mount embryos fixed with 4% paraformaldehyde was detected by TUNEL using the In Situ Cell Death Detection Kit (Roche) following the manufacturer's protocol. For the quantification of TUNEL-positive cells, at least four embryos per condition were analyzed as described above.

Microarray Analysis

Control and ATG morphant embryos were sampled at 72 hpf and RNA samples were obtained from pools of 20 embryos per condition and three pooled biologic replicates of control and ATG morphants were analyzed. Single-color microarray-based gene expression analysis was performed using an Agilent Technologies (Santa Clara, CA, USA) custom oligo microarray 4 × 44 K with eArray design ID 021626 and containing in total 43,371 probes of a 60-oligonucleotide length. Total RNA was amplified and labeled with Cy3 dye using the single-color Low Input Quick Amp Labeling kit (Agilent) following the manufacturer's indications using 200 ng of RNA in each reaction. Next, 1,65 μg of labeled cRNA were hybridized to the arrays. Overnight hybridization (17 hours, 65 °C and 10 rpm rotation) was performed in a Microrarray Hybridization Oven (Agilent). After hybridization, microrarrays were washed with Gene Expression Wash Buffers 1 and 2 (Agilent Technologies) and scanned using the High-Resolution C Scanner (Agilent). Feature Extraction Software 10.7.3.1 (Agilent) was used for spot to grid alignment, feature extraction and quantification. Processed data were subsequently imported into GeneSpring GX 11.5 (Agilent). Significance cutoffs for the ratios of control versus ATG morpholino were set at 1.5-fold change at $P < 0.05$ (sample *t*-test), respectively, for differentially expressed genes (DEGs). For the DEGs, gene IDs were converted to human ENSEMBL gene IDs using g:orth function from G:profiler (http://biit.cs.ut.ee/gprofiler), taking advantage of the more complete gene ontology annotations of the human genes and improving, in this way, the subsequent analysis of the functional categories. The complete microarray data have been deposited in NCBI's Gene Expression Omnibus and are accessible through GEO Series accession number GSE57836 (http://www.ncbi.nlm.nih.gov/geo/query/acc.cgi?acc = GSE57836). Gene ontology enrichment analysis was performed using Database for Annotation, Visualization, and Integrated Discovery (DAVID) software tools (http://david.abcc.ncifcrf.gov), and the resulting categories were considered significant at $P < 0.05$.

Quantitative Real-Time Polymerase Chain Reaction

Ribonucleic acid was isolated with TRIzol (Life Technologies), DNAse treated with RQ1 DNAse (Promega) and reverse transcribed using Superscript III (Life Technologies). For the quantification of mRNA expression levels, quantitative PCR was performed. cDNA was diluted 1:25 for target genes and 1:2,000 for *rps18*, and used as a template. The reactions (20 μL final volume) contained 10 μL of SYBR GreenER qPCR SuperMix (Life Technologies), 500 nmol/L of forward and reverse primers and 5 μL of cDNA. Reactions were run in a MyiQ Real-Time PCR Detection System (Bio-Rad, Madrid, Spain) using the following protocol: 2 minutes at 50 °C, 8 minutes at 95 °C, followed by 40 cycles of 15 seconds denaturation at 95 °C and 30 seconds at the corresponding melting temperatures, and a final melting curve of 81 cycles from 55 °C to 95 °C (0.5 °C increments every 10 seconds). Samples were run in triplicate and fluorescence was measured at the end of every extension step. Fluorescence readings were used to estimate the values for the threshold cycles. Primer sequences are shown in Supplementary Table 1.

Maintenance of MIN6 Cells

MIN6 pancreatic β-cells were kindly provided by Dr Albert Barbera (IDIBAPS, Barcelona, Spain). Cells were maintained at 37 °C (95% O_2, 5% CO_2) in Dulbecco's Modified Eagle's medium supplemented with 15% heat-inactivated fetal bovine serum and 100 U/mL penicillin per 0.1 mg/mL streptomycin. Medium was changed every 2 to 3 days. MIN6 cells used in the present study were collected at passages 31 to 38.

Generation of a Zebrafish glut2 Expression Construct and Transient Transfection of MIN6 Cells

The full-length sequence of the zebrafish *glut2* cDNA[9] was amplified by PCR and subcloned in pcDNA3 vector containing enhanced GFP (green fluorescent protein). Approximately 1×10^5 cells/well were plated in 12-well plates and transfected 24 hours later at a confluence of 70 to 80% with Lipofectamine 2000 (Life Technologies) following the manufacturer's indications. Cells were stimulated and/or lysed at 48 hours post transfection. Overexpression experiments were performed by transfecting 2 μg/well of *zfglut2*-GFP construct. Cells were lysed 24 hours post transfection. Mock controls were transfected only with lipofectamine and cultured in the same conditions as other transfected cells.

In Vitro Glucose Uptake Assays

MIN6 cells were washed twice with HEPES-buffered saline and incubated with HEPES-buffered saline containing 50 μmol/L 2-deoxyglucose [0.5 μCi/mL 2-[3H]-deoxyglucose (2-[3H]-DG)] for 30 minutes at room temperature. After this period, the transport solution was removed and cells were rinsed three times with ice-cold PBS containing 50 mmol/L D-glucose. Finally, cells were lysed with 0.05 N NaOH, and the radioactivity was determined by scintillation counting using a β-counter (Packard Bioscience, Meriden, CT, USA). Nonspecific uptake was carried out in the presence of 50 μmol/L cytochalasin B in the transport solution, and these values were subtracted from all other values. Glucose uptake was measured in triplicate, normalized to total protein and expressed as fold induction with respect to nonstimulated cells.

Glucose Measurements

Glucose measurements were performed using a fluorescence-based enzymatic detection kit (Biovision Inc., Milpitas, CA, USA).

Statistical Analysis

Results are expressed as mean ± s.e. Statistical differences were analyzed by Kruskal–Wallis and Mann–Whitney nonparametric tests and considered to be significant at $P < 0.05$.

RESULTS

Zebrafish *glut2* is Expressed in the Developing Brain, Liver, Pronephric Tubules, and Endocrine Pancreas

We first determined the localization of the expression of zebrafish *glut2* during early development by *in situ* hybridization (ISH). At 24 hpf, *glut2* expression was localized in the telencephalon, eyes, hindbrain, and pronephric duct (Figures 1A and 1B). By 48 hpf, strong expression of *glut2* was observed in the head and in the pronephric duct (Figure 1C). At 72 and 120 hpf, *glut2* appeared expressed in the liver, pronephric tubules, anterior intestine, and endocrine pancreas (Figures 1E, 1E′, 1F, 1F′, 1H, 1H′, 1I, 1I′), as demonstrated by the colocalization of preproinsulin, a specific marker for this tissue (Figure 1I, inset). At 72 and 120 hpf, *glut2* was also expressed in the hindbrain, specifically in the cerebellum and medulla oblongata (Figures 1D, 1D′, 1G, 1G′).

Knockdown of Zebrafish *glut2* Disrupts Brain Development

To study the function of *glut2* during the early development in zebrafish, we investigated the effects of abrogation of *glut2* by using two different antisense morpholinos, one to inhibit translation at the start methionine (ATG MO) and a second one designed to interfere with splicing between exons 5 and 6 (splice MO) that code for transmembrane helix 6, an important structure for the glucose transport activity of class I GLUTs. Embryos injected with the ATG MO showed a severe delay in the development of the embryo, mainly in the brain area. Morphant embryos at 24 hpf showed less developed eyes and a dense mass was observed in the brain area instead of the hindbrain ventricle, causing the loss of the midbrain/hindbrain structures (Figures 2D and 2E). Embryos injected with the splice MO appeared to be a phenocopy of the ATG morphants, confirming the specificity of the morpholino (Figures 2G and 2H). By 48 hpf, morphant embryos displayed a defective formation and enlargement of the hindbrain ventricle associated with anterior displacement of the telencephalon (Figures 2F and 2I). Morphant embryos did not survive past 96 to 120 hpf. The incidence of the morphant phenotype was 95.9 ± 1.4% ($n = 765$) in embryos injected with the ATG MO and 93.4 ± 1.2% ($n = 536$) in embryos injected with the splice MO. Furthermore, we confirmed the extent of the splice blocking activity of the splice MO at different stages throughout development in *glut2* morphants. Analysis of *glut2* mRNA transcripts by reverse transcription PCR from embryos injected with the splice MO revealed the appearance of aberrant splice products from 24 hpf until 96 hpf (Supplementary Figure 1) although the efficiency of the morpholino appeared to decrease at 96 hpf. To further demonstrate the specificity of the *glut2* morphant phenotype, we performed rescue experiments by co-injecting the ATG MO or splice MO with the rat *Glut2* or zebrafish *glut2* mRNA, respectively, lacking the morpholino target sequences (Figure 3). Our results show that rat *Glut2* mRNA was able to rescue the phenotype in ATG morphant embryos (Figures 3A, 3B, 3D, 3F, 3G, and 3I) and that zebrafish *glut2* mRNA was able to rescue the phenotype in splice morphant embryos (Figures 3A, 3C, 3E, 3F, 3H, and 3J). To demonstrate the functionality of the zebrafish *glut2* mRNA in the rescue of the splice morphants, we examined glucose uptake under basal conditions in MIN6 cells transfected with a zebrafish *glut2* expression construct. MIN6 cells overexpressing zebrafish *glut2* showed a significant increase in glucose uptake compared with control cells (Supplementary Figure 2). Taken together, these results show that *glut2* knockdown affects brain development in zebrafish embryos.

Defective Glucose Uptake in *glut2*-Deficient Embryos

To evaluate the functional consequence of *glut2* abrogation on glucose metabolism, we performed glucose uptake experiments using 2-NBDG, a non-metabolizable fluorescently labeled glucose analog. We observed a significant decrease in 2-NDBG uptake in the head and body in ATG morphant embryos, with most of the glucose remaining inside the yolk (Figures 4d, 4e, 4g, and 4h). In contrast, ATG morphants rescued with rat *Glut2* mRNA recovered glucose uptake as evidenced by the significant increase in the amount of fluorescent glucose signal in the head and the body and by the significant decrease in fluorescence in the yolk when compared with ATG morphant embryos, yielding a similar 2-NBDG distribution than control embryos (Figure 4B). In addition, to further characterize the defect in glucose homeostasis, we measured free glucose levels in *glut2*-deficient embryos. Our results show that ATG morphant embryos presented lower levels of free glucose at 24 hpf (Supplementary Figure 3). These results strongly suggest that *glut2* morphant embryos may be experiencing hypoglycemia due to the observed reduction in glucose uptake from the yolk.

Knockdown of *glut2* Influences Brain Development in Zebrafish by Affecting Cerebellar Progenitor Cells

In view of the severe alterations in the hindbrain structure as a result of *glut2* abrogation, we set out to further characterize this phenotype in the central nervous system (CNS) by performing immunohistochemical analyses using an antibody against neuron-specific acetylated tubulin. In control embryos, a basic axon scaffold had formed in the embryonic zebrafish brain by 24 hpf, consisting of two bilaterally symmetric longitudinal tracts connected by commissures, providing a template for subsequent development (Figures 5i and 5i′). In contrast, the neuronal architecture of *glut2* morphants was clearly altered, revealing thinner, poorly fasciculated longitudinal tracts (Figures 5ii and 5ii′). ATG morphant embryos co-injected with rat *Glut2* mRNA

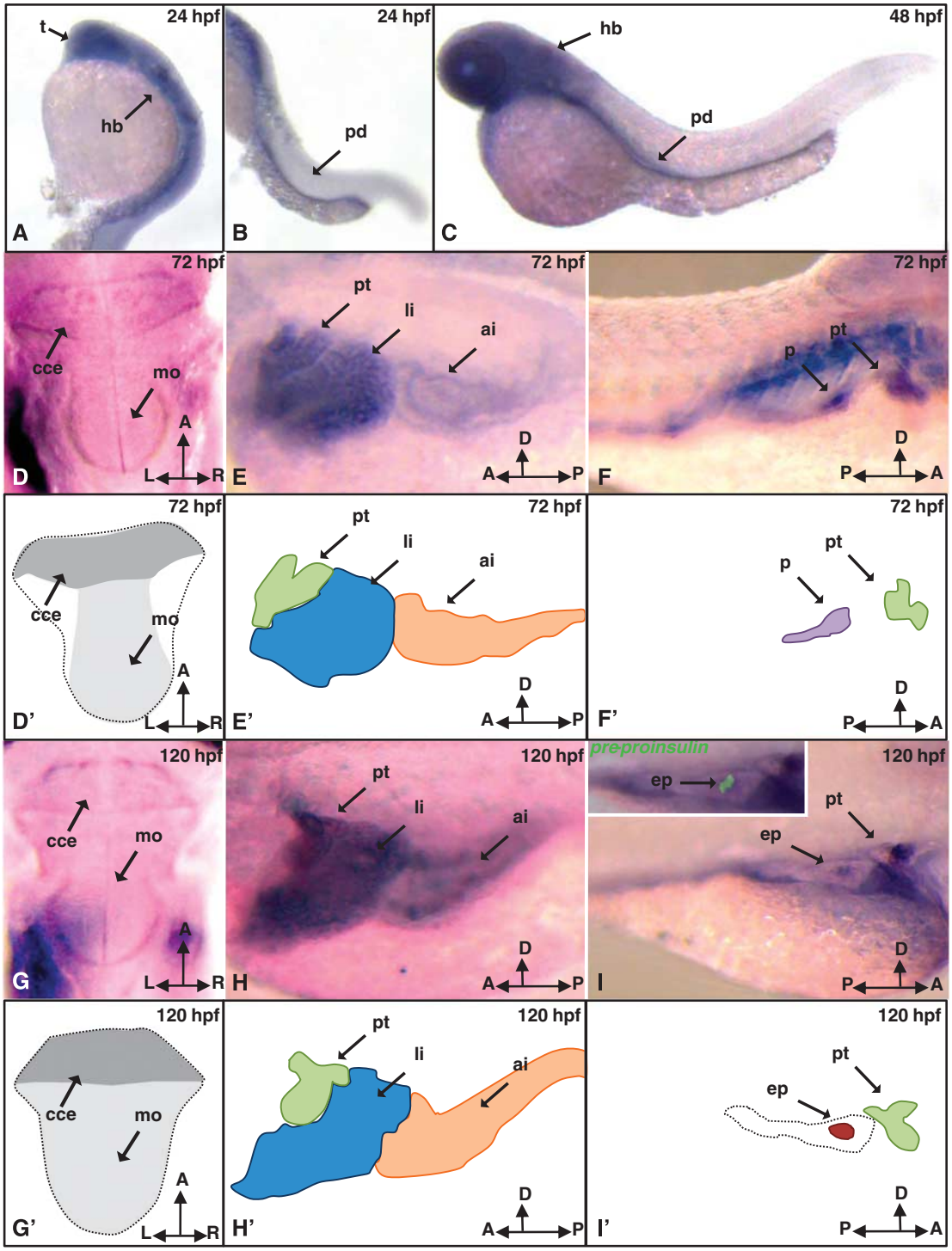

Figure 1. Localization of the expression of *glut2* in zebrafish. Whole-mount *in situ* hybridization showing expression of zebrafish *glut2* mRNA at 24 hours post fertilization (hpf; **A** and **B**), 48 hpf (**C**), 72 hpf (**D**–**F**), and 120 hpf (**G**–**I**). Left (**A**–**C**, **E**, and **H**), right lateral views (**F** and **I**), and dorsal views of the hindbrain region (**D** and **G**) are shown. To confirm *glut2* expression in endocrine pancreas, double *in situ* hybridization showing *pre-proinsulin* expression was performed (**I**, inset). (**D'**–**I'**) Schematic representations of **D**–**I** highlighting with different colors the regions where *glut2* is expressed. Black dotted contours outline the hindbrain region (**D'** and **G'**) and the pancreas (**I'**). Anterior intestine (ai), corpus cerebelli (cce), endocrine pancreas (ep), hindbrain (hb), liver (li), medulla oblongata (mo), pronephric duct (pd), pronephric tubule (pt), telencephalon (t).

recovered the brain structure similar to control embryos (Figures 5iii and 5iii'). Surprisingly, control and ATG morphant embryos showed no significant differences in axonal structure at 48 hpf (data not shown).

To assess the effects of *glut2* abrogation in the hindbrain region, we performed ISH for various proneural genes: *ptf1a*, *atoh1b*, *atoh1c*, and *neurod*. *ptf1a* is a marker of progenitor cells of GABAergic neurons in the ventricular zone.[10] *atoh1b* and *atoh1c*

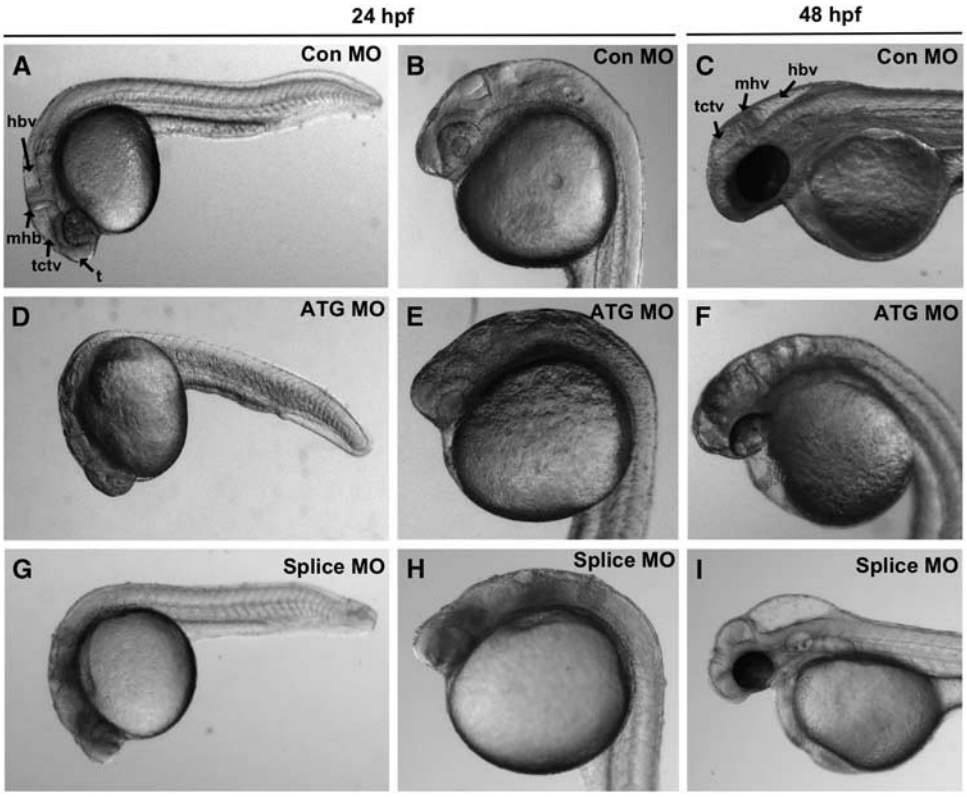

Figure 2. *glut2* abrogation disrupts brain development. Phenotype of embryos injected with a control morpholino (Con MO) at 24 hours post fertilization (hpf; **A** and **B**) and at 48 hpf (**C**), a morpholino targeting the translational start site (ATG MO) at 24 hpf (**D** and **E**), and at 48 hpf (**F**) and a morpholino targeting the splice acceptor between exons 5 and 6 (Splice MO) at 24 hpf (**G** and **H**) and at 48 hpf (**I**). Embryos injected with both morpholinos displayed a defective formation of the hindbrain that could be observed from 24 hpf onwards. Hindbrain ventricle (hbv), midbrain/hinbrain boundary (mbh), tectal ventricle (tctv), telencephalon (t).

are markers of progenitor cells of glutamatergic neurons whereas *neurod* is a marker of immature and mature granule cells.[10] Embryos injected with ATG MO lacked expression of *ptf1a* at 24 hpf and their expression pattern at 48 hpf was similar to that in control embryos at 24 hpf (Figures 5A–5F). Similarly, *atoh1b* showed a marked delay in its pattern of expression in ATG morphants at 24 and 48 hpf (Figures 5G–5L). In contrast, ATG morphants showed no significant alteration in *neurod* expression at 24 and 48 hpf (Figures 5M–5R). At 72 hpf, however, the pattern of expression of *atoh1b, neurod*, and *atoh1c*, first expressed at this stage, was not different between control and ATG morphants (Supplementary Figure 4). Moreover, ATG morphant embryos rescued with rat *Glut2* mRNA recovered normal expression patterns of *atoh1b* and *ptf1a* (Supplementary Figure 5).

Loss of *glut2* Leads to an Increase in Apoptotic Cell Death

On the basis of the observed expression of *glut2* in the hindbrain and on the consequences of *glut2* abrogation in this brain region, we hypothesized that the loss of *glut2* in zebrafish embryos could affect the incidence of cell death. Examination of cell death in ATG morphant embryos at 24 hpf using the vital dye acridine orange showed a significant increase (1.6-fold, $P < 0.05$) in cell death, primarily in the brain area, over control embryos (Figures 6A–6C and 6G). ATG morphants co-injected with rat *Glut2* mRNA presented similar levels of cell death as control embryos (Figures 6D and 6G). To determine whether the observed increase in cell death in *glut2* morphant embryos corresponded to apoptotic cell death, we performed TUNEL assays and observed a significantly higher number of apoptotic cells present in the hindbrain of *glut2* morphants compared to control embryos at 24 hpf (Figures 6E, 6F, and 6H).

Transcriptome Profiling of *glut2* Morphants Evidences Changes in the Expression of Genes Involved in Neural Processes and Apoptosis

To study the effects of *glut2* abrogation on gene expression in zebrafish embryos, we performed a transcriptome analysis of zebrafish ATG morphant embryos at 72 hpf and compared it with control embryos. Microarray analysis was performed setting significance cutoffs at 1.5-fold change at $P < 0.05$ (sample *t*-test). A total of 1,912 genes (DEGs) were found to be regulated in *glut2* morphant embryos: 1,025 upregulated and 887 downregulated genes. A set of 11 selected DEGs were validated by quantitative PCR (Supplementary Table 2). Next, to better characterize the annotated DEGs, we performed a gene ontology analysis for functional classification (Supplementary Table 3). Analysis of Gene Ontology-Biological Process revealed a significant enrichment in functional categories involved in neural processes (e.g., neuron projection, neurotransmitter metabolic process, and visual perception), programmed cellular death (e.g., apoptosis and cell death), patterning, muscle development, immune processes, and response to hypoxia/oxygen levels in *glut2* morphant embryos. Among DEGs involved in neural development, several genes known to participate in the organization and maintenance of the mid-hindbrain boundary (*eng2b, fgf13a, her8.2, pax2b*), as well as in glutamate and glycine neurotransmission (*grin1b* and *glra4a*) were downregulated in *glut2* morphant embryos (Table 1). Furthermore, marker genes for GABAergic neurons (*pvalb7, aldca*),

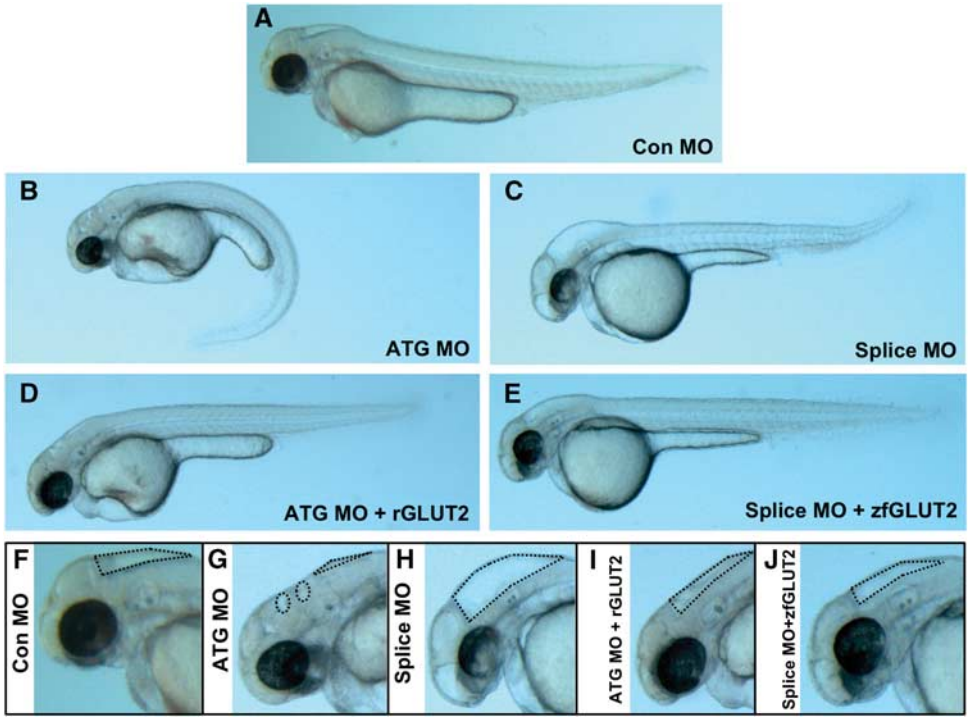

Figure 3. Morphant phenotype caused by abrogation of *glut2* can be rescued with full-length zebrafish *glut2* and rat GLUT2 mRNA. Phenotype of embryos injected with a control morpholino (Con MO) at 48 hpf (**A**), ATG morpholino (ATG MO) at 48 hpf (**B**) and splice morpholino (Splice MO) at 48 hpf (**C**). Rescue of overall morphant phenotype at 48 hpf by co-injection of ATG MO with rat GLUT2 mRNA (rGLUT2; **D**) and of Splice MO with zebrafish *glut2* (zfGLUT2; **E**). (**F**–**J**) Shows higher magnification images of the cephalic region of Con MO (**F**), ATG MO (**G**), Splice MO (**H**), rescued ATG morphants (**I**), and rescued splice morphants (**J**). The hindbrain region (outlined by black dotted line) is affected in the morphants (**G** and **H**), while brain development in rescued embryos (**I** and **J**) is similar to that observed in control embryos (**F**).

glutamatergic neurons (*atoh8, zic2a, tbr1b*), and neural stem cells (*sox2*) were upregulated in *glut2* morphant embryos. Also coincident with the increased apoptosis in *glut2* morphant embryos, several pro-apoptotic genes (*aifm1,bnip3lb, badb, cideb, cdip1, dram*) were found to be upregulated. A number of genes related to insulin/IGF-I signaling were also downregulated (e.g., *insra, irs1, ifg1rb, igf2bp1, mtor, mapk1, mapk14b, pik3r2*) in *glut2* morphant embryos. In addition, the expression of genes involved in the bone morphogenetic protein/wnt pathways (*bmp4, tgfb1a, fsta, fstb, dvl1a, dvl3a, wnt16, and wif1*) were significantly altered in embryos lacking *glut2*. Not surprisingly, the mRNA expression levels of *glut2* (*slc2a2)* as well as that of *transferrin* (*tfa*) and *pdx1*, marker genes for the *glut2*-expressing tissues liver and endocrine pancreas, respectively, were significantly decreased in *glut2* morphant embryos (Table 1, Supplementary Table 2).

DISCUSSION

In this study we describe a vertebrate model of GLUT2 deficiency. Using a reverse genetic approach, we have knocked down *glut2* expression in zebrafish embryos causing disorganization of the hindbrain, severe mispatterning of axonal scaffolds, and alterations in the development of the neural progenitor cells. Furthermore, we have related these observed functional consequences of *glut2* depletion to a reduction in glucose uptake and availability and, consequently, to an increase in programmed cell death in the brain region.

Expression analysis of zebrafish embryos by ISH showed that *glut2* is expressed in the liver, pronephric tubules, anterior intestine, endocrine pancreas, and importantly, in the hindbrain, particularly in the corpus cerebelli and medulla oblongata. In mammals, GLUT2 expression has been reported in the cerebellum, brain nuclei, hypothalamic nuclei, neurons, glial cells, and astrocytes,[4,11–15] where GLUT2 is believed to be expressed in glucose sensing neurons that regulate feeding behavior, energy metabolism, and glucose homeostasis.[3] Therefore, the similar neural localization of the expression of *glut2* in zebrafish is indicative of the existence of a glucose sensing region in the zebrafish brain.

Despite current data strongly linking GLUT2 to central glucose sensing in the mammalian brain, little is known on the importance of GLUT2 in the development of the CNS. In the present study, we show that abrogation of *glut2* expression during early development in zebrafish had critical consequences in the formation of the CNS. The *glut2* morphant embryos showed severe alterations in the formation of the hindbrain ventricle, affecting the midbrain-hindbrain structures. In view of the coinciding neurodegenerative morphant phenotype and the localization of *glut2* expression in the hindbrain at early developmental stages, we hypothesized that abrogation of *glut2* may have affected the development of neural progenitor cells. In zebrafish, as in mammals, neurons are classified into two major groups: the excitatory glutamatergic, and the inhibitory GABAergic neurons.[16] In the mouse, glutamatergic neurons derived from progenitor cells located in the upper rhombic lip express the proneural gene Atoh1,[17] whereas the glutamatergic immature and mature granule cells express the proneural gene NeuroD that is required for their generation and differentiation.[18] On the other hand, murine GABAergic neurons are derived from progenitor cells expressing the proneural gene Ptf1a.[19] Recently, it has been shown that the neurogenic processes of both glutamatergic and GABAergic neurons are conserved between mammals and zebrafish and that the above-mentioned proneural genes are also specifically expressed in progenitor cells of the hindbrain region in zebrafish.[10] Here, we show that abrogation of *glut2* caused important alterations in the expression

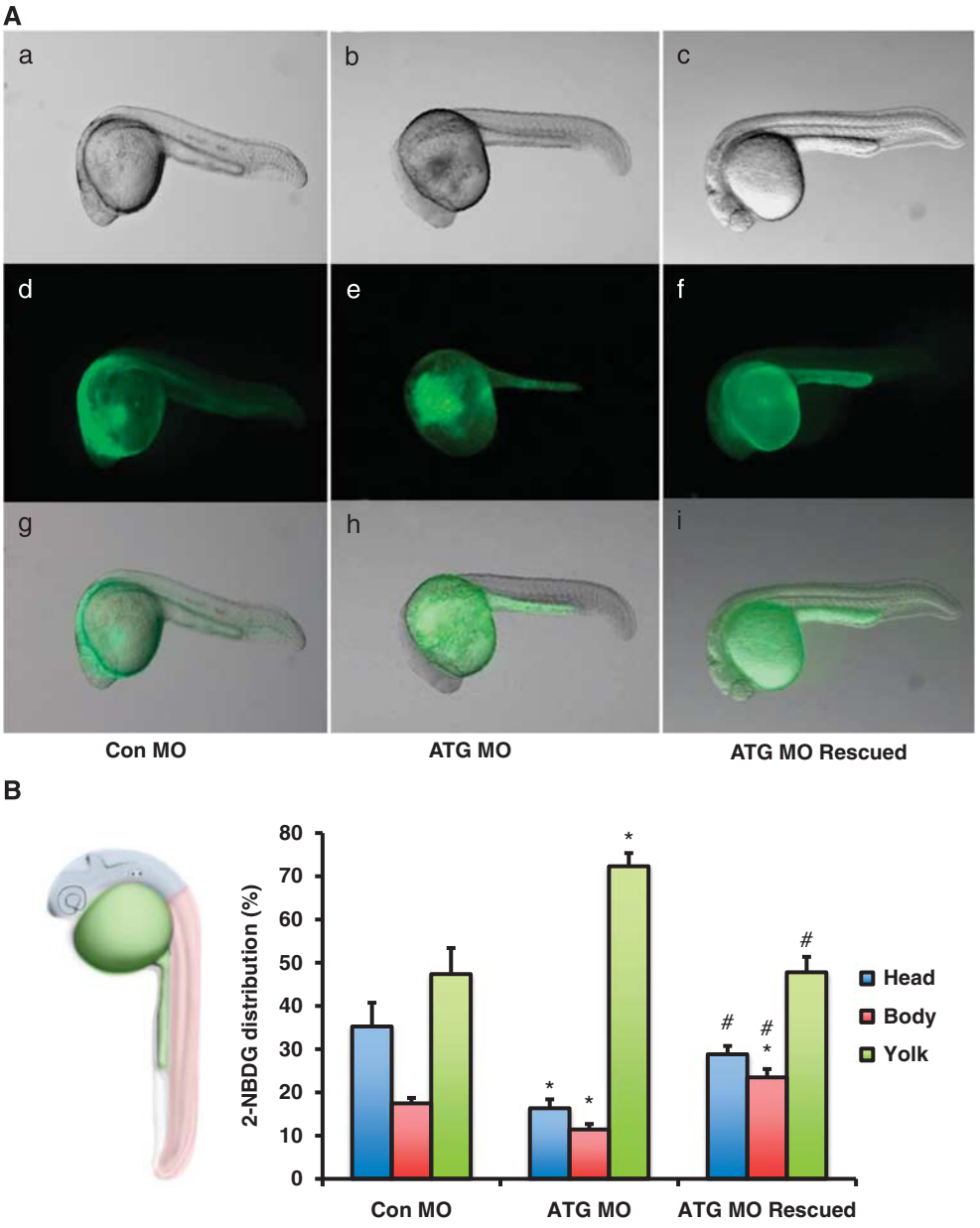

Figure 4. Knockdown of *glut2* results in inhibition of glucose uptake *in vivo*. (**A**) (**a**–**i**) Bright field (upper line, **a**–**c**), fluorescent (middle line, **d**–**f**), and overlay (bottom line, **g**–**i**) pictures of control, ATG morphants, and rescued embryos at 24 hpf. (**B**) Measurement of fluorescent signal in embryos injected with 2-NBDG. Control injected embryos (**a**, **d**, and **g**) displayed significant amounts of fluorescent glucose throughout the embryo; in contrast, ATG morphants (**b**, **e**, and **h**) showed very minimal fluorescent glucose visible at 60 minutes after injection. Embryos injected with ATG MO+rat GLUT2 mRNA (ATG MO Rescued) recovered glucose uptake to levels similar to Con MO (**c**, **f**, and **i**). * indicates significant differences compared with the Con MO injected embryos ($^{*}P < 0.05$; $^{**}P < 0.01$; $^{***}P < 0.001$). # indicates significant differences compared with ATG MO injected embryos ($^{\#\#}P < 0.01$; $^{\#\#\#}P < 0.001$).

pattern of proneural marker genes in the hindbrain region during early development in zebrafish. First, *glut2* morphant embryos showed a significant delay in the expression pattern of *ptf1a,* indicating that abrogation of *glut2* may have affected the development of *ptf1a*-expressing cells from the ventricular zone, reported in mice to be the source of all GABAergic neurons in the cerebellum.[19] Second, *glut2* morphant embryos showed altered expression pattern of *atoh1b* as well as an alteration of the upper rhombic lip region at 24 and 48 hpf. Altered expression of ionotropic NMDA glutamate and glycine receptors (*grin1b* and *glra4a*, respectively) in *glut2* morphant embryos further suggest that the connectivity of *ptf1a*- and *atoh1b*-expressing neurons could also be affected. Interestingly, abrogation of *glut2* induced the expression of known marker genes of Purkinje (*pvalb7* and *aldca*), granule (*atoh8, zic2a* and *tbr1b*), and neural stem cells (*sox2*), suggesting that a compensatory mechanism to the alterations in hindbrain structure may have taken place at 72 hpf. Furthermore, the observed alteration of the hindbrain structure in *glut2* morphant embryos was related to a severe alteration of the neural scaffold, as evidenced by acetylated tubulin immunostaining, and to the downregulation of the expression of genes that participate in the establishment of the mid-hindbrain boundary and the patterning of the hindbrain (*eng2b*, *pax2b*, *fgf13a*, and *her8.2*)[16] at 24 hpf. Therefore, abrogation of *glut2* disrupted hindbrain development and, specifically, the development of progenitors for GABAergic and glutamatergic

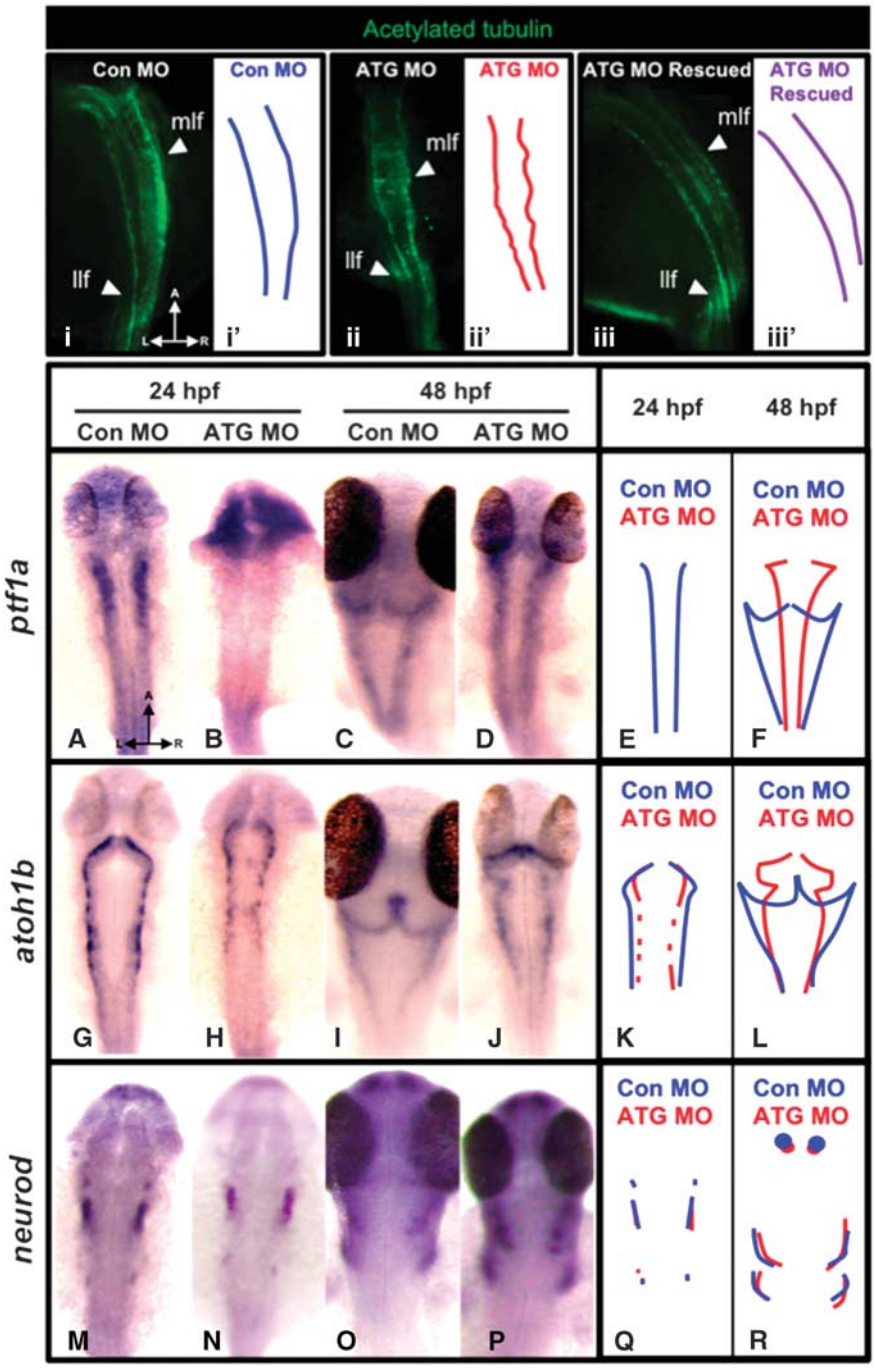

Figure 5. *glut2* abrogation causes hindbrain disorganization and affects the expression of cerebellar proneural genes. To study the consequences of *glut2* knockdown in the hindbrain structure we performed immunostaining using an antibody against acetylated tubulin in con MO, ATG MO, and ATG MO+rat GLUT2 mRNA rescued embryos at 24 hpf (i, ii, iii). At this stage, morphant embryos showed disorganized axon tracts. Rescued embryos showed a hindbrain structure similar to control injected embryos. Lateral longitudinal fascicles (llf); medial longitudinal fascicles (mlf). To further study the consequences of *glut2* abrogation in the neural progenitor cells we performed ISH for the proneural genes *ptf1a* (**A**–**D**), *atoh1b* (**G**–**J**), *neurod* (**M**–**P**) in control injected embryos at 24 hpf (**A**, **G**, and **M**), and 48 hpf (**C**, **I**, and **O**), and in ATG morphants at 24 hpf (**B**, **H**, and **N**) and 48 hpf (**D**, **J**, and **P**). To better illustrate the effects caused by the abrogation of *glut2*, immunostained medial longitudinal fascicles have been outlined (i', ii', iii'). The expression patterns observed by ISH of the proneural genes are represented with diagrams overlapping the expression patterns in control and ATG morphants at 24 hpf and 48 hpf of *ptf1a* (**E** and **F**), *atoh1b* (**K** and **L**), and *neurod* (**Q** and **R**). A, anterior; L, left; R, right.

neurons in the zebrafish hindbrain. Overall, these results clearly indicate that *glut2* is an important factor for neurodevelopment in the zebrafish embryo.

Here, we also show that abrogation of *glut2* expression in zebrafish embryos resulted in a significant reduction in whole-body glucose uptake and in a decrease in cell viability due to apoptotic cell death mainly in the brain region. It is known that the entry and utilization of glucose in cells can act as important mediators of cell survival, linking glucose availability with cellular viability, as is well described in cancer cells.[20]

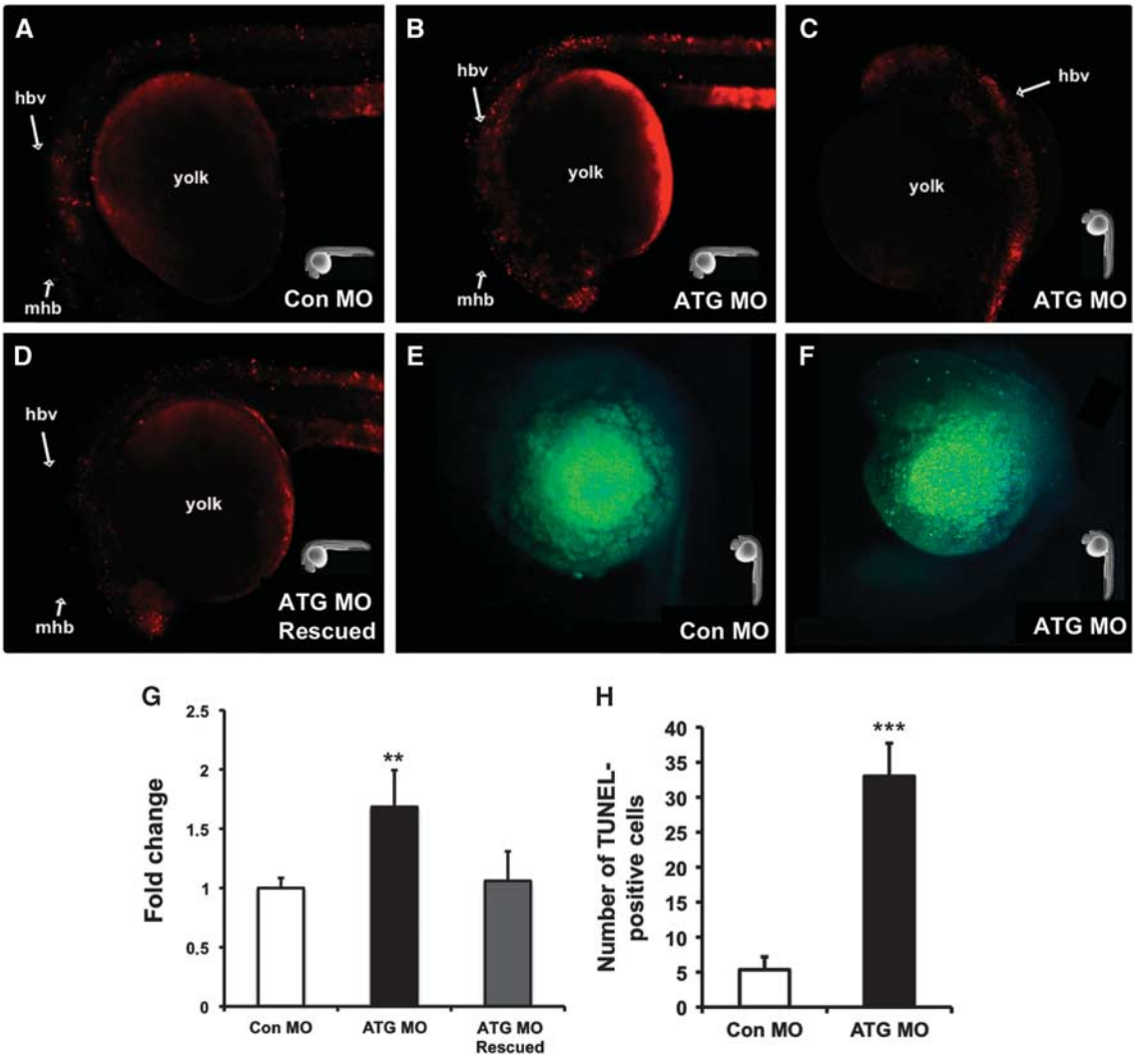

Figure 6. Abrogation of *glut2* enhances cell death mainly in the head region. To assay for cell death, embryos injected with control morpholino (Con MO; **A**), ATG morpholino (ATG MO; **B** and **C**), and ATG MO+rat GLUT2 mRNA (ATG MO Rescued; **D**) were stained with the vital dye acridine orange. To assay for apoptosis, embryos injected with Con MO (**E**) and ATG MO (**F**) were analyzed by TUNEL assay. At 24 hpf, there was an overall increase in cell death and apoptosis primarily localized in the hindbrain region (**B**, **C**, and **F**). Fluorescent signal analysis (**G**) and counting of TUNEL-positive cells (**H**) confirmed a significant increase in cell death and apoptosis, respectively, in ATG morphants which appears reverted in rescued embryos (**G**). * indicates significant differences compared with the Con MO injected embryos (**$P < 0.01$; ***$P < 0.001$). Hindbrain ventricle (hbv), midbrain/hindbrain boundary (mbh), telencephalon (t). In the images (**A**–**F**), the position of the embryos is indicated by a representation of a zebrafish embryo.

In neurons, glucose deprivation induces apoptosis that can be reverted by the enhancement of GLUT1 expression by IGF-1,[21] an important neural survival factor[22] that blocks the activity of the pro-apoptotic factor Bad through the PI3K/Akt pathway.[23] Recently, a link between glucose homeostasis and apoptosis has been established in *glut1*-deficient and *akt2*-deficient zebrafish embryos, two *in vivo* models of altered glucose homeostasis that showed increased apoptosis and an almost identical neurodegenerative phenotype that could be rescued by abrogation of *bad*.[24,25] In the present study, we provide evidence supporting the hypothesis that the decrease in glucose availability caused by *glut2* abrogation, as evidenced by the reduction in glucose uptake and the ensuing hypoglycemia, may have induced apoptosis in zebrafish embryos, leading to neurodegeneration. On one hand, expression of rat *Glut2* in *glut2* morphant embryos restored glucose uptake and decreased the incidence of cell death, rescuing the morphant phenotype. On the other hand, *glut2* abrogation resulted in the upregulation of the expression of *bad* and several other pro-apoptotic factors. Interestingly, a number of components of the insulin/IGF-I signaling pathway were down-regulated in *glut2* morphant embryos, suggesting that this important survival pathway was suppressed as a result of glucose deprivation due to *glut2* abrogation. Furthermore, the expression of *igfbp1a*, a marker of decreased glucose availability[26] that is transcriptionally repressed by insulin and that causes defects in brain development when overexpressed[27], was upregulated in *glut2* morphant embryos, supporting the hypoglycemic phenotype. Therefore, we propose that the decrease in glucose uptake and availability in *glut2* morphant zebrafish embryos may have led to a reduction in the production of survival signals through the insulin/IGF-1 signaling pathway and/or the production of glucose metabolites and, consequently, to an increase in apoptotic cell death. Our results support the notion that glucose is essential for cell survival in the CNS in zebrafish and that glucose transporters

Table 1. Selection of differentially expressed genes in *glut2* morphant zebrafish embryos

Gene name	*Description*	*FC*	*P*	*Gene name*	*Description*	*FC*	*P*
Neural function				*Apoptosis*			
aldoca	Aldolase C, fructose-bisphosphate, a	2.12	0.044	*aifm1*	Apoptosis-inducing factor, mitochondrion-assoc. 1	−1.63	0.008
atoh8	Atonal homolog 8	4.52	0.000	*apitd1*	Apoptosis-inducing, TAF9-like domain 1	−1.60	0.028
cdh1	Cadherin 1, epithelial	2.01	0.002	*bnip3lb*	BCL2/adenovirus E1B interacting protein 3-like b	1.56	0.040
eng2b	Engrailed 2b	−1.58	0.048	*badb*	BCL2-antagonist of cell death b	1.56	0.018
fgf13a	Fibroblast growth factor 13a	−2.01	0.003	*bag5*	BCL2-associated athanogene 5	−3.53	0.005
foxa3	Forkhead box A3	−1.52	0.012	*cideb*	Cell death-inducing DFFA-like effector b	2.98	0.004
foxb1b	Forkhead box B1b	−1.79	0.000	*cdip1*	Cell death-inducing p53 target 1	−1.54	0.015
grin1b	Glutamate receptor, ionotropic, NMDA 1b	−2.55	0.017	*dram1*	DNA-damage regulated autophagy modulator 1	3.38	0.020
glra4a	Glycine receptor, alpha 4a	−2.11	0.013	*irf1b*	Interferon regulatory factor 1b	3.22	0.046
her8.2	Hairy-related 8.2	−2.03	0.015	*irf3*	Interferon regulatory factor 3	−2.68	0.005
her9	Hairy-related 9	1.51	0.010	*perp*	PERP, TP53 apoptosis effector	−1.80	0.015
hoxa13a	Homeo box A13a	−1.66	0.048	*pdcd4b*	Programmed cell death 4b	3.44	0.016
hoxb1a	Homeo box B1a	−1.72	0.025	*tp63*	Tumor protein p63	−1.66	0.050
hoxb3a	Homeo box B3a	−2.12	0.037	*faim2a*	Fas apoptotic inhibitory molecule 2a	−1.61	0.014
hoxb5b	Homeo box B5b	−1.51	0.002				
hoxb6a	Homeo box B6a	−1.56	0.046	*Metabolism*			
hoxb6b	Homeo box B6b	−1.96	0.026	*pfkfb3*	6-phosphofructo-2-kinase/fructose-2,6-biphosphatase 3	1.78	0.032
hoxb9a	Homeo box B9a	−1.58	0.028	*fabp10a*	Fatty acid-binding protein 10a, liver basic	2.69	0.015
hoxc1a	Homeo box C1a	−1.51	0.029	*fabp6*	Fatty acid-binding protein 6, ileal (gastrotropin)	5.73	0.041
hoxc8a	Homeo box C8a	−1.50	0.044	*gpd1l*	Glycerol-3-phosphate dehydrogenase 1-like	−1.67	0.043
hoxd11a	Homeo box D11a	−1.63	0.004	*lepr*	Leptin receptor	1.77	0.040
hoxd13a	Homeo box D13a	−1.82	0.000	*lpin1*	Lipin 1	1.83	0.029
ngrn	Neugrin, neurite outgrowth associated	1.58	0.024	*lpl*	Lipoprotein lipase	1.56	0.004
nrxn1a	Neurexin 1a	−1.82	0.008	*npy8ar*	Neuropeptide Y receptor Y8a	2.62	0.022
nrxn2b	Neurexin 2b	−2.01	0.026	*ppargc1b*	PPAR, gamma, coactivator 1, beta	−1.89	0.009
nos1	Nitric oxide synthase 1 (neuronal)	−3.77	0.016	*pfkma*	Phosphofructokinase, muscle a	1.68	0.020
pax2b	Paired box gene 2b	−1.94	0.012	*pygmb*	Phosphorylase, glycogen (muscle) b	−1.66	0.006
pax3a	Paired box gene 3a	1.54	0.019	*slc2a2*	Solute carrier family 2, member 2	−2.52	0.048
pvalb7	Parvalbumin 7	2.26	0.004	*soga1*	Suppressor of glucose, autophagy associated 1	−2.42	0.000
sox2	SRY-box containing gene 2	1.99	0.001	*ucp1*	Uncoupling protein 1	1.81	0.028
tbr1b	T-box, brain, 1b	2.09	0.014	*ucp3*	Uncoupling protein 3	3.92	0.020
Insulin action and signaling				*Nodal pathway*			
eif4ebp3	Eukaryotic translation initiation factor 4E BP3	1.72	0.006	*lft2*	Lefty2	1.61	0.001
insra	Insulin receptor a	−1.54	0.005	*pdcb*	Phosducin b	2.17	0.022
irs1	Insulin receptor substrate 1	−1.77	0.003	*bmp4*	Bone morphogenetic protein 4	−1.52	0.030
igf1rb	Insulin-like growth factor 1b receptor	−1.63	0.006				
igf2bp1	Insulin-like growth factor 2 mRNA binding protein 1	−1.60	0.044	*Wnt pathway*			
igfbp1a	Insulin-like growth factor binding protein 1a	1.58	0.009	*dvl1a*	Dishevelled, dsh homolog 1a (Drosophila)	−1.66	0.049
mtor	Mechanistic target of rapamycin	−1.98	0.007	*dvl2*	Dishevelled, dsh homolog 2 (Drosophila)	−1.65	0.025
map3k7	Mitogen activated protein kinase kinase kinase 7	−1.70	0.034	*dvl3a*	Dishevelled, dsh homolog 3a (Drosophila)	−1.63	0.033
mapk1	Mitogen-activated protein kinase 1	−1.52	0.026	*wnt16*	Wingless-type MMTV integration site family, 16	1.62	0.020
mapk14b	Mitogen-activated protein kinase 14b	−1.73	0.023	*wif1*	Wnt inhibitory factor 1	−3.52	0.000
mapk8b	Mitogen-activated protein kinase 8b	−1.92	0.011				
map2k4b	Mitogen-activated protein kinase kinase 4b	−1.69	0.019	*Others*			
map2k5	Mitogen-activated protein kinase kinase 5	−1.63	0.039	*fsta*	Follistatin a	1.50	0.019
map2k6	Mitogen-activated protein kinase kinase 6	−1.76	0.024	*fstb*	Follistatin b	1.58	0.016
pdx1	Pancreatic and duodenal homeobox 1	−1.64	0.008	*gata5*	GATA-binding protein 5	−2.13	0.028
pik3r4	Phosphoinositide-3-kinase, regulatory subunit 4	1.50	0.002	*sox19b*	SRY-box containing gene 19b	1.68	0.017
pik3r2	Phosphoinositide-3-kinase, regulatory subunit 2	−1.77	0.007	*sox2*	SRY-box containing gene 2	1.99	0.001
prkcbb	Protein kinase C, beta b	−1.64	0.011	*sox6*	SRY-box containing gene 6	5.69	0.048
prkcq	Protein kinase C, theta	11.3	0.031	*sox9b*	SRY-box containing gene 9b	−2.04	0.036
socs1a	Suppressor of cytokine signaling 1a	3.10	0.000	*thrb*	Thyroid hormone receptor beta	−2.23	0.009
tfr1b	Transferrin receptor 1b	−1.60	0.002	*tgfb1a*	Transforming growth factor, beta 1a	−2.75	0.016
tfa	Transferrin-a	−1.74	0.003				

Control and morphant embryos were used for gene expression analysis using a zebrafish oligonucleotide microarray (GPL13390). Data are shown as fold change (FC). *P*: *P* value.

have a key role in this process. In addition to Glut2 and Glut1, that is expressed astrocytes and in the blood–brain barrier allowing the entry of glucose into the brain from the circulation, the mammalian brain expresses primarily Glut3, a high affinity GLUT that is expressed in neurons, but also Glut4, Glut5, and Glut8 at lower levels.[1,28] In view of the complexity of the GLUT system in the brain, further studies will be required to elucidate the specific role of the different GLUTs expressed in the brain.

Given that abrogation of *glut2* resulted in increased apoptosis primarily in the brain region, we hypothesize that glucose deprivation-induced apoptosis in the hindbrain of *glut2* morphants may have been responsible for the observed disruption of hindbrain organization and, specifically, for the alterations in the development of progenitors for GABAergic and glutamatergic neurons in the embryonic zebrafish hindbrain. At the present time, we cannot ascertain if *glut2* abrogation may have induced apoptosis specifically in GABAergic and glutamatergic precursors nor if these effects may have been direct or indirect through other *glut2*-expressing cells. This leads to the important question of where specifically *glut2* is expressed in the zebrafish brain, a question that has not been completely resolved even in mammals. In the mammalian brain, GLUT2 is expressed in glucose sensitive neurons in the hypothalamus and in the brainstem[29] but the exact nature of GLUT2-expressing neurons (i.e., GABAergic or glutamatergic) in the central glucose sensing system has been poorly described to date, although there is evidence indicating that GABA release in neurons is regulated by glucose.[30,31] GABAergic neurons in the ventromedial hypothalamus are inactivated when glucose levels decrease under hypoglycemic conditions, enhancing the counterregulatory response to hypoglycemia.[32] These observations suggest the possibility that GLUT2-expressing neurons in structures belonging to the central glucose sensing system could be, at least in part, GABAergic neurons. Supporting these observations, Glut2 has recently been shown to be expressed in a homogenous glucose-sensing subpopulation of GABAergic neurons in the nucleus of the tractus solitarius in mice.[33] Unfortunately, our attempts at localizing *glut2* in *ptf1a*- and *atoh1b*-expressing cells were unsuccessful due to the low levels of expression of *glut2* in the zebrafish brain, as in mammals.[34] Approaches involving genetic labeling of *glut2*-expressing cells will be required to identify the nature of cells that express *glut2* in the zebrafish brain in future studies.

It is worth noting that the functional consequences of abrogating *glut1*[24] or *glut2* (this study) in zebrafish are both severe and very similar, particularly when considering that the effects of *glut2* abrogation occur in the absence of changes in the expression of *glut1* (data not shown). A possible explanation for the apparently similar function of *glut1* and *glut2* in early zebrafish development may lie in possible differences in their pattern of expression that would allow for transporter-specific glucose availability in different key brain areas during early development. Recently, it was reported that morpholinos could cause non-specific apoptosis and changes in the expression of proneural marker genes by activation of p53.[35] However, our data on the ability of rat *Glut2* mRNA to rescue the apoptotic morphant phenotype (Figure 6), on the similar phenotype generated by the two different morpholinos used (Figures 2 and 3) and on the lack of changes in the mRNA expression levels of *p53* and its downstream targets *mdm2* and *p21* in *glut2* morphant embryos (data not shown), strongly argue against the possibility of off-target effects of the morpholinos in our study.

Interestingly, *glut2* morphant embryos showed altered expression of receptors for leptin (*lepr*) and NPY (*npy8ar*) as well as of uncoupling proteins 1 and 3 (*ucp1*, *ucp3*), suggesting that some of the factors known to participate in the GLUT2-mediated control of feeding and thermoregulation in mammals[29] are also dependent on the presence of a functional *glut2* gene in zebrafish. Although *ucp1* is obviously not involved in thermoregulation in zebrafish but may instead reduce ATP production, these observations add to those on the localization of *glut2* in the zebrafish hindbrain in support of the hypothesis that a central glucose sensing mechanism involving *glut2* may be present in the zebrafish brain, providing a novel and useful experimental model for investigating the role of GLUT2 in glucose sensing in the brain. Furthermore, consistent with the expression of GLUT2 in liver and endocrine pancreas, *glut2* abrogation decreased the expression of *tfa* and *pdx1*, two well-known marker genes for these important tissues in glucose metabolism. In particular, *pdx1* is necessary for the proper regulation of the glucose-dependent insulin secretion by β-cells[36] and for pancreas development in zebrafish since *pdx1*-null zebrafish lack this organ.[37] Hence, the downregulation of *pdx1* expression suggests that the glucose-responsive regulation of insulin synthesis in endocrine pancreas could be affected as a consequence of the abrogation of *glut2* in zebrafish. Interestingly, genetic inactivation of *Glut2* specifically in the nervous system was recently shown to reduce pancreatic β-cell mass and proliferation and suppress first-phase insulin secretion due to decreased parasympathetic activity in mice, supporting the notion of a central function for GLUT2 in glucose homeostasis.[34] At this time, it is not known if the decrease in the expression of *pdx1* in zebrafish *glut2* morphant embryos could be the result of the abrogation of the expression of *glut2* in the pancreas, or in the brain, or in both.

To summarize, in the present study we provide evidence for the physiological role of *glut2* in glucose homeostasis. Importantly, we demonstrate that *glut2* is essential for the development of neural progenitors for GABAergic and glutamatergic neurons, suggesting the existence of a glucose-sensing region in the zebrafish brain. We propose that the lack of *glut2* in specific brain areas in the zebrafish embryo results in glucose deprivation causing increased apoptotic cell death that we believe is the underlying cause for the observed alterations in brain development. Importantly, the observed phenotype in *glut2* morphant embryos shows certain similarities with FBS patients. Like *glut2* morphants, FBS patients that are diagnosed during their infancy exhibit growth delay and impaired glucose homeostasis that is characterized by fasting hypoglycemia and hypergalactosemia.[2] In some cases, hepatomegaly is also observed as a consequence of glycogen accumulation, a process that becomes exacerbated during infancy.[2] Unfortunately, we were not able to assess whether abrogation of *glut2* in zebrafish also affected liver glycogen levels because we failed to detect glycogen in the liver in zebrafish embryos up to 72 hpf (data not shown). It is possible that the developmental stage of the studied embryos may have been too early to be able to appreciate glycogen accumulation in the liver, resembling the human situation. However, the mRNA expression levels of glycogen phosphorylase (*pygmb*), an enzyme involved in glycogen breakdown, were decreased in *glut2* morphant embryos, suggesting that glycogen metabolism may have been altered in zebrafish embryos as a result of *glut2* abrogation. This is supported by reports indicating that deficiency of this enzyme in the liver is responsible for glycogen storage disease type VI, characterized by hepatomegaly and growth retardation.[38] On the other hand, cases diagnosed with FBS include patients with delayed psychomotor development.[39] Interestingly, psychomotor delay has been associated with alterations in the cerebellar development in humans at early ages.[40] Our findings that *glut2* is expressed in the zebrafish cerebellum and that the development of the cerebellum is altered in *glut2* morphant embryos indicates that our *glut2*-deficiency model recapitulates yet another phenotype of FBS patients. In conclusion, our study demonstrates the physiological importance of *glut2* in glucose uptake and availability during brain development and provides a novel model system for the study of diseases derived from GLUT2-deficient states, representing an attractive tool for the development of new drug or genetic therapies for the treatment of FBS.

DISCLOSURE/CONFLICT OF INTEREST

The authors declare no conflict of interest.

ACKNOWLEDGMENTS

The authors thank Dr Cristina Pujades and Dr Javier Terriente (Universitat Pompeu Fabra, Barcelona, Spain) for their generous assistance with *in situ* hybridization and for critically reading the manuscript (C. Pujades). The authors also thank Purificación Márquez for assistance with glucose uptake assays.

REFERENCES

1 Mueckler M, Thorens B. The SLC2 (GLUT) family of membrane transporters. *Mol Aspects Med* 2013; **34**: 121–138.
2 Santer R, Steinmann B, Schaub J. Fanconi-Bickel syndrome--a congenital defect of facilitative glucose transport. *Curr Mol Med* 2002; **2**: 213–227.
3 Marty N, Dallaporta M, Thorens B. Brain glucose sensing, counterregulation, and energy homeostasis. *Physiology (Bethesda)* 2007; **22**: 241–251.
4 Marty N, Dallaporta M, Foretz M, Emery M, Tarussio D, Bady I *et al.* Regulation of glucagon secretion by glucose transporter type 2 (glut2) and astrocyte-dependent glucose sensors. *J Clin Invest* 2005; **115**: 3545–3553.
5 Eny KM, Wolever TM, Fontaine-Bisson B, El-Sohemy A. Genetic variant in the glucose transporter type 2 is associated with higher intakes of sugars in two distinct populations. *Physiol Genomics* 2008; **33**: 355–360.
6 Wan HZ, Hulsey MG, Martin RJ. Intracerebroventricular administration of antisense oligodeoxynucleotide against GLUT2 glucose transporter mRNA reduces food intake, body weight change and glucoprivic feeding response in rats. *J Nutr* 1998; **128**: 287–291.
7 Bady I, Marty N, Dallaporta M, Emery M, Gyger J, Tarussio D *et al.* Evidence from glut2-null mice that glucose is a critical physiological regulator of feeding. *Diabetes* 2006; **55**: 988–995.
8 Stolarczyk E, Guissard C, Michau A, Even PC, Grosfeld A, Serradas P *et al.* Detection of extracellular glucose by GLUT2 contributes to hypothalamic control of food intake. *Am J Physiol Endocrinol Metab* 2010; **298**: E1078–E1087.
9 Castillo J, Crespo D, Capilla E, Díaz M, Chauvigné F, Cerdà J *et al.* Evolutionary structural and functional conservation of an ortholog of the GLUT2 glucose transporter gene (SLC2A2) in zebrafish. *Am J Physiol Regul Integr Comp Physiol* 2009; **297**: R1570–R1581.
10 Kani S, Bae YK, Shimizu T, Tanabe K, Satou C, Parsons MJ *et al.* Proneural gene-linked neurogenesis in zebrafish cerebellum. *Dev Biol* 2010; **343**: 1–17.
11 Arluison M, Quignon M, Nguyen P, Thorens B, Leloup C, Penicaud L. Distribution and anatomical localization of the glucose transporter 2 (GLUT2) in the adult rat brain--an immunohistochemical study. *J Chem Neuroanat* 2004; **28**: 117–136.
12 Roncero I, Alvarez E, Chowen JA, Sanz C, Rabano A, Vazquez P *et al.* Expression of glucose transporter isoform GLUT-2 and glucokinase genes in human brain. *J Neurochem* 2004; **88**: 1203–1210.
13 Kang L, Routh VH, Kuzhikandathil EV, Gaspers LD, Levin BE. Physiological and molecular characteristics of rat hypothalamic ventromedial nucleus glucosensing neurons. *Diabetes* 2004; **53**: 549–559.
14 Leloup C, Arluison M, Lepetit N, Cartier N, Marfaing-Jallat P, Ferre P *et al.* Glucose transporter 2 (GLUT 2): expression in specific brain nuclei. *Brain Res* 1994; **638**: 221–226.
15 Nualart F, Godoy A, Reinicke K. Expression of the hexose transporters GLUT1 and GLUT2 during the early development of the human brain. *Brain Res* 1999; **824**: 97–104.
16 Hibi M, Shimizu T. Development of the cerebellum and cerebellar neural circuits. *Dev Neurobiol* 2012; **72**: 282–301.
17 Alder J, Cho NK, Hatten ME. Embryonic precursor cells from the rhombic lip are specified to a cerebellar granule neuron identity. *Neuron* 1996; **17**: 389–399.
18 Miyata T, Maeda T, Lee JE. NeuroD is required for differentiation of the granule cells in the cerebellum and hippocampus. *Genes Dev* 1999; **13**: 1647–1652.
19 Hoshino M, Nakamura S, Mori K, Kawauchi T, Terao M, Nishimura YV *et al.* Ptf1a, a bHLH transcriptional gene, defines GABAergic neuronal fates in cerebellum. *Neuron* 2005; **47**: 201–213.
20 Mjiyad El N, Caro-Maldonado A, Ramirez-Peinado S, Munoz-Pinedo C. Sugar-free approaches to cancer cell killing. *Oncogene* 2011; **30**: 253–264.
21 Russo VC, Kobayashi K, Najdovska S, Baker NL, Werther GA. Neuronal protection from glucose deprivation via modulation of glucose transport and inhibition of apoptosis: a role for the insulin-like growth factor system. *Brain Res* 2004; **1009**: 40–53.
22 Torres-Aleman I, Pons S, Arevalo MA. The insulin-like growth factor I system in the rat cerebellum: developmental regulation and role in neuronal survival and differentiation. *J Neurosci Res* 1994; **39**: 117–126.
23 Datta SR, Dudek H, Tao X, Masters S, Fu H, Gotoh Y *et al.* Akt phosphorylation of BAD couples survival signals to the cell-intrinsic death machinery. *Cell* 1997; **91**: 231–241.
24 Jensen PJ, Gitlin JD, Carayannopoulos MO. GLUT1 deficiency links nutrient availability and apoptosis during embryonic development. *J Biol Chem* 2006; **281**: 13382–13387.
25 Jensen PJ, Gunter LB, Carayannopoulos MO. Akt2 modulates glucose availability and downstream apoptotic pathways during development. *J Biol Chem* 2010; **285**: 17673–17680.
26 Cotterill AM, Holly JM, Amiel S, Wass JA. Suppression of endogenous insulin secretion regulates the rapid rise of insulin-like growth factor binding protein (IGFBP)-1 levels following acute hypoglycaemia. *Clin Endocrinol (Oxf)* 1993; **38**: 633–639.
27 Murphy LJ, Rajkumar K, Molnar P. Phenotypic manifestations of insulin-like growth factor binding protein-1 (IGFBP-1) and IGFBP-3 overexpression in transgenic mice. *Prog Growth Factor Res* 1995; **6**: 425–432.
28 Vannucci SJ, Maher F, Simpson IA. Glucose transporter proteins in brain: delivery of glucose to neurons and glia. *Glia* 1997; **21**: 2–21.
29 Mounien L, Marty N, Tarussio D, Metref S, Genoux D, Preitner F *et al.* Glut2-dependent glucose-sensing controls thermoregulation by enhancing the leptin sensitivity of NPY and POMC neurons. *FASEB J* 2010; **24**: 1747–1758.
30 Levin BE. Glucose-regulated dopamine release from substantia nigra neurons. *Brain Res* 2000; **874**: 158–164.
31 During MJ, Leone P, Davis KE, Kerr D, Sherwin RS. Glucose modulates rat substantia nigra GABA release in vivo via ATP-sensitive potassium channels. *J Clin Invest* 1995; **95**: 2403–2408.
32 Zhu W, Czyzyk D, Paranjape SA, Zhou L, Horblitt A, Szabo G *et al.* Glucose prevents the fall in ventromedial hypothalamic GABA that is required for full activation of glucose counterregulatory responses during hypoglycemia. *Am J Physiol Endocrinol Metab* 2010; **298**: E971–E977.
33 Lamy CM, Sanno H, Labouèbe G, Picard A, Magnan C, Chatton J-Y *et al.* Hypoglycemia-activated GLUT2 neurons of the nucleus tractus solitarius stimulate vagal activity and glucagon secretion. *Cell Metab* 2014; **19**: 527–538.
34 Tarussio D, Metref S, Seyer P, Mounien L, Vallois D, Magnan C *et al.* Nervous glucose sensing regulates postnatal β cell proliferation and glucose homeostasis. *J Clin Invest* 2014; **124**: 413–424.
35 Gerety SS, Wilkinson DG. Morpholino artifacts provide pitfalls and reveal a novel role for pro-apoptotic genes in hindbrain boundary development. *Dev Biol* 2011; **350**: 279–289.
36 MacFarlane WM, Read ML, Gilligan M, Bujalska I, Docherty K. Glucose modulates the binding activity of the beta-cell transcription factor IUF1 in a phosphorylation-dependent manner. *Biochem J* 1994; **303**(Pt 2):625–631.
37 Yee NS, Yusuff S, Pack M. Zebrafish pdx1 morphant displays defects in pancreas development and digestive organ chirality, and potentially identifies a multipotent pancreas progenitor cell. *Genesis* 2001; **30**: 137–140.
38 Wolfsdorf JI, Weinstein DA. Glycogen storage diseases. *Rev Endocr Metab Disord* 2003; **4**: 95–102.
39 Aperia A, Bergqvist G, Linne T, Zetterstrom R. Familial Fanconi syndrome with malabsorption and galactose intolerance, normal kinase and transferase activity. A report on two siblings. *Acta Paediatr Scand* 1981; **70**: 527–533.
40 Ventura P, Presicci A, Perniola T, Campa MG, Margari L. Mental retardation and epilepsy in patients with isolated cerebellar hypoplasia. *J Child Neurol* 2006; **21**: 776–781.

Supplementary Information accompanies the paper on the Journal of Cerebral Blood Flow & Metabolism website (http://www.nature.com/jcbfm)